

Title	Deposition of copper by plasma-enhanced atomic layer deposition using a novel N-Heterocyclic carbene precursor
Authors	Coyle, Jason P.;Dey, Gangotri;Sirianni, Eric R.;Kemmell, Marianna L.;Yap, Glenn P. A.;Ritala, Mikko;Leskela, Markku;Elliott, Simon D.;Barry, Seán T.
Publication date	2013-03
Original Citation	Jason P. Coyle, Gangotri Dey, Eric R. Sirianni, Marianna L. Kemell Glenn P. A. Yap, Mikko Ritala, Markku Leskela, Simon D. Elliott Sean T. Barry (2013). Deposition of Copper By Plasma-Enhanced Atomic Layer Deposition Using a Novel N-Heterocyclic Carbene Precursor. Chemistry of Materials, 25 (7), pp 1132–1138. DOI: 10.1021/cm400215q
Type of publication	Article (peer-reviewed)
Link to publisher's version	<a href="http://pubs.acs.org/doi/abs/10.1021/cm400215q">http://pubs.acs.org/doi/abs/10.1021/cm400215q</a> - <a href="http://pubs.acs.org/doi/abs/10.1021/cm400215q">10.1021/cm400215q</a>
Rights	© 2013, American Chemical Society. This document is the Accepted Manuscript version of a Published Work that appeared in final form in Chemistry of Materials, copyright © American Chemical Society after peer review and technical editing by the publisher. To access the final edited and published work see <a href="http://pubs.acs.org/doi/abs/10.1021/cm400215q">http://pubs.acs.org/doi/abs/10.1021/cm400215q</a>
Download date	2025-02-03 18:01:56
Item downloaded from	<a href="https://hdl.handle.net/10468/1056">https://hdl.handle.net/10468/1056</a>



# UCC

**University College Cork, Ireland**  
Coláiste na hOllscoile Corcaigh

**Deposition of Copper By Plasma-Enhanced Atomic Layer  
Deposition Using a Novel N-Heterocyclic Carbene Precursor**

Journal:	<i>Chemistry of Materials</i>
Manuscript ID:	Draft
Manuscript Type:	Article
Date Submitted by the Author:	n/a
Complete List of Authors:	Coyle, Jason; Carleton University, Chemistry Dey, Gangotri; Tyndall National Institute, Electronic Theory Group Sirianni, Eric; University of Delaware, Department of Chemistry Kemell, Marianna; University of Helsinki, Department of Chemistry Yap, Glenn; University of Delaware, Chemistry & Biochemistry Ritala, Mikko; University of Helsinki, Chemistry Leskela, Markku; University of Helsinki, Department of Chemistry Elliott, Simon; Tyndall National Institute, Barry, Sean; Carleton University, Chemistry

SCHOLARONE™  
Manuscripts

## Deposition of Copper By Plasma-Enhanced Atomic Layer Deposition Using a Novel N-Heterocyclic Carbene Precursor

Jason P. Coyle<sup>1</sup>, Gangotri Dey<sup>2</sup>, Eric R. Sirianni<sup>3</sup>, Marianna L. Kemell<sup>4</sup>, Glenn P. A. Yap<sup>3</sup>, Mikko Ritala<sup>4</sup>, Markku Leskelä<sup>4</sup>, Simon D. Elliott<sup>2</sup>, Sean T. Barry<sup>1\*</sup>

<sup>1</sup> Department of Chemistry, Carleton University, 1125 Colonel By Drive, Ottawa, K1S 5B6, Canada. E-mail: sean\_barry@carleton.ca; Tel: +1 613-520-2600.

<sup>2</sup> Tyndall National Institute, University College Cork, Dyke Parade, Cork, Ireland.

<sup>3</sup> Department of Chemistry & Biochemistry, University of Delaware, Newark, DE 19716, USA.

<sup>4</sup> Laboratory of Inorganic Chemistry, Department of Chemistry, University of Helsinki P.O. Box 55, FI-00014 Helsinki, Finland.

### Abstract

Two novel N-heterocyclic carbene (NHC)-containing copper(I) amides are reported as atomic layer deposition (ALD) precursors. 1,3-diisopropyl-imidazolin-2-ylidene copper hexamethyldisilazide (**1**) and 4,5-dimethyl-1,3-diisopropyl-imidazol-2-ylidene copper hexamethyldisilazide (**2**) were synthesized and structurally characterized. The thermal behaviour of both compounds was studied by thermogravimetric analysis (TGA), and they were both found to be reasonably volatile compounds. Compound **1** had no residual mass in the TGA and showed long-term stability at temperatures as high as 130 °C, while **2** had a residual mass of 7.4 %. Copper metal with good resistivity was deposited using **1** by plasma-enhanced atomic layer deposition. The precursor demonstrated self-limiting behaviour indicative of ALD, and gave a growth rate of 0.2 Å/cycle. Compound **2** was unsuccessful as an ALD precursor under similar conditions. Density functional theory calculations showed that both compounds adsorb dissociatively onto a growing copper film as long as there is some atomic roughness, via cleavage of the Cu-carbene bond.

### Introduction

Copper metal remains an interesting topic for chemical vapour deposition (CVD) and atomic layer deposition (ALD) due to its use in microelectronics, primarily as an interconnect.<sup>1</sup> Several potential copper(I) and copper(II) precursors have been reported for chemical vapor deposition (CVD) and atomic layer deposition (ALD), including  $\beta$ -diketonates,<sup>2</sup>  $\beta$ -diketiminates,<sup>3</sup> amidinates,<sup>4</sup> guanidates,<sup>5</sup> aminoalkoxides,<sup>6</sup> and pyrrolylaldiminates.<sup>7</sup> Of these precursors, the exclusively N-bonded ligands are interesting due to their lack of Cu-O bonds, making them less susceptible to oxygen inclusion in the deposited copper film as well as in the barrier and adhesion layers.

ALD has been proposed as an alternative method to CVD for depositing conformal, ultra-thin films at comparatively lower temperatures. ALD is similar to CVD except that the substrate is sequentially exposed to one reactant at a time, or one dose of a reactant at a time. Conceptually, it is a simple process: a first reactant is introduced to a heated substrate whereby it forms a monolayer on the surface of the substrate. Excess reactant is pumped out (e.g., evacuated). Next a second reactant is introduced and reacts with the existing monolayer to form a sub-monolayer of a desired reaction product through a self-limiting surface reaction. The process is self-limiting since the deposition reaction halts once the initially adsorbed (physisorbed or chemisorbed) monolayer of the first reactant has fully reacted with the second reactant. Finally, the excess second reactant is evacuated. This sequence constitutes one

1  
2  
3  
4  
5 deposition cycle. The desired film thickness is obtained by repeating deposition cycles as necessary. As  
6 is apparent, the sequential layer-by-layer nature of ALD has the disadvantage of being slower than  
7 some other deposition techniques. However it is this cycle of building up highly uniform layers one at  
8 a time that allows ALD to produce films of a surface uniformity, smoothness and thinness that is  
9 impossible to achieve with other techniques. This makes ALD uniquely valuable in demanding coating  
10 applications. In the specific application of ALD used for this study, the “second reactant” in this case is  
11 a hydrogen plasma, generated remotely from the growing surface from dihydrogen carried by argon.  
12 This plasma is screened by a grounded grid, filtering out ions from the plasma, and permitting only the  
13 radicals (and light) produced in the plasma to impinge on the surface. The role of the the hydrogen  
14 plasma is to scour off the ligand system, as well as reducing the copper surface species to metal. Given  
15 the complex nature of the plasma, the mechanistic reaction at the surface is likely complex. An  
16 excellent review of plasma ALD processes can be found here.<sup>8</sup>  
17  
18

19  
20 It is interesting that copper amides have not been prevalent precursors for ALD. It is known that  
21 copper(I) amides typically produce a tetrameric structure,<sup>9</sup> and copper(I) amides are more thermally  
22 stable than alkyl or alkoxo species.<sup>10</sup> Thus, it has been difficult to isolate a thermally stable copper  
23 amide precursor that exhibits sufficient volatility to be considered for CVD or ALD. However,  
24 monomeric copper(I) species are well-studied in catalysis. Specifically, copper(I) NHCs are well-  
25 known to exhibit good thermal stability during C-H bond activation<sup>11</sup> and can drastically increase the  
26 thermal stability in sensitive Cu(I) species.<sup>12,13</sup> Thus, the synthesis and thermal characterization of  
27 copper(I) amides stabilized by NHCs was undertaken to examine their suitability as ALD precursors.  
28 This design strategy is common for group 11 precursors, and recent success has been shown for the  
29 plasma enhanced ALD of Ag films.<sup>14</sup>  
30  
31

32  
33 Herein is reported novel copper(I) NHCs: 1,3-diisopropyl-imidazolin-2-ylidene copper  
34 hexamethyldisilazide (**1**) and 4,5-dimethyl-1,3-diisopropyl-imidazol-2-ylidene copper  
35 hexamethyldisilazide (**2**) (Scheme 1). The choice of ligands was paramount for the design of this new  
36 copper precursor. Preliminary screening showed that hexamethyldisilazide (N(SiMe<sub>3</sub>)<sub>2</sub>) provided  
37 excellent thermal stability to Cu(I), where alkyl amides are known to allow plating of copper metal.<sup>10</sup> It  
38 was less clear from the outset whether an unsaturated NHC (imidazol-2-ylidene) or saturated NHC  
39 (imidazolin-2-ylidene) would allow for better precursor properties and for better metal deposition.  
40 Preliminary screening of unsaturated NHCs showed that a imidazol-2-ylidene with a methyl-substituted  
41 backbone provided a more thermally stable copper compound than an unsubstituted imidazol-2-  
42 ylidene. Preliminary screening showed backbone substitution of imidazolin-2-ylidenes proved to be  
43 unnecessary as such NHCs afforded copper compounds with sufficient thermal stability. Interestingly,  
44 our preliminary screening led us to choose NHCs with different stabilities towards dimerization; the  
45 dimer from the carbene in **2** is unknown, whereas the dimer from the carbene in **1** is a volatile olefin.<sup>15</sup>  
46  
47  
48

49  
50 Some Cu(I) precursors are well known to undergo disproportionation reactions to Cu(0) and Cu(II),  
51 which has been exploited in the CVD of copper metal films.<sup>16</sup> This process relies on the clean purging  
52 from the deposition zone of the Cu(II) product along with any stabilizing Lewis base employed in the  
53 Cu(I) precursor. Cu(II) hexamethyldisilazide compounds are unknown and Cu(II) amide compounds  
54 are exceptionally rare.<sup>17</sup> The attempted synthesis of Cu[N(SiMe<sub>3</sub>)<sub>2</sub>]<sub>2</sub> results in the isolation of  
55 [CuN(SiMe<sub>3</sub>)<sub>2</sub>]<sub>4</sub>.<sup>18</sup> CVD of copper metal films from [CuN(SiMe<sub>3</sub>)<sub>2</sub>]<sub>4</sub> have been reported at 200°C under  
56 a flow of H<sub>2</sub> without any indication of a disproportionation component to film growth.<sup>18</sup> Both of the  
57 NHCs used in **1** and **2** are volatile at room temperature when not coordinated; however their affinities  
58 for a copper surface are investigated herein.  
59  
60

1  
2  
3  
4  
5  
6 Additionally, explicit atomic-scale insight into ALD chemistry has been obtained through simulations  
7 using Density Functional Theory (DFT).<sup>19</sup> Most DFT studies have been related to the ALD of binary  
8 compounds such as HfO<sub>2</sub><sup>20</sup> and Al<sub>2</sub>O<sub>3</sub>,<sup>21</sup> but there are relatively few simulations on the ALD of pure  
9 metals (e.g. Ni<sup>22</sup> and Co<sup>23</sup>). Possible Cu ALD reactions have been computed by Mårtensson et al. for  
10 CuCl as the precursor and H<sub>2</sub><sup>24</sup> as the reducing agent. The formation of Cu from amidinate<sup>25</sup> and β-  
11 diketonate<sup>26,27</sup> based precursors has also been simulated. Recently, Dey et al. have computed a detailed  
12 mechanism for Cu ALD using ZnEt<sub>2</sub> as the reducing agent,<sup>28</sup> following experiments by Lee et al.<sup>29</sup> Here  
13 we use DFT to compare the probable adsorption mechanism of the carbene-based Cu precursors **1** and  
14 **2**.  
15  
16

## 17 Results and Discussion

18  
19  
20 Both compounds can be made by simple salt metathesis from the NHC copper chloride and  
21 Et<sub>2</sub>O·LiN(SiMe<sub>3</sub>)<sub>2</sub>. The resulting <sup>1</sup>H spectra were simple and reflected the expected formulations in  
22 both cases. Compound **1** easily underwent sublimation under reduced atmosphere at 90 °C, and was  
23 sublimed quantitatively. It melted at 51 °C, which is beneficial for a vapour phase precursor: having  
24 the precursor as a liquid during the deposition process ensures a uniform production of vapour pressure.  
25 Thermogravimetric analysis (TGA) showed the onset of volatility at 91 °C and a residual mass of 0 %  
26 (Figure 1, black trace). Compound **2** could also be quantitatively sublimed at 95 °C and had a melting  
27 point of 119 °C. TGA showed an onset of volatility at 87 °C, but with a residual mass of 7.4 %. Since  
28 the mass of copper in **2** comprises 15.72 % of the total molecular mass, this compound was possibly  
29 undergoing volatilization and decomposition over the thermal range of the TGA.  
30  
31  
32

33 It was possible to isolate crystals of both **1** and **2** that were sufficient for structural analysis (Figure 2,  
34 Table 1). In both cases, the copper is in a linear geometry with the ligands staggered and roughly  
35 orthogonal. The Cu-N bonds (1.84 Å for **1** and 1.87 Å for **2**) are shorter than reported for the copper(I)  
36 hexamethyldisilazide tetramer (1.92 – 1.93 Å),<sup>18</sup> but similar to copper alkyl amide compounds.<sup>9</sup> The  
37 longer amide contact in **2** might be due to the steric bulk of the backbone methyl groups forcing the  
38 carbene's isopropyl groups to orient toward the amide moiety, in turn forcing back the amide group.  
39 The copper-carbon bonds fall in the range of other monomeric, linear N-bonded Cu-NHC  
40 complexes,<sup>30,12</sup> suggesting that the shortened Cu-N bond might be due to enhanced backbonding to the  
41 copper. This also suggests that the copper amide bond might be stabilized to cleavage upon adsorption  
42 of the compound at a growing copper surface, suggesting that the carbene will be lost upon  
43 chemisorption.  
44  
45  
46

47 A “stepped isotherm” TGA was employed to establish the evaporation rate and vapour pressures of  
48 these compounds. A stepped isotherm is a thermogravimetric experiment where the temperature is  
49 ramped by 10 °C and held for 10 minutes while the compound volatilizes; the number of steps gives  
50 the number of data points from which a Clausius-Clapeyron curve can be constructed. This experiment  
51 can be used to relate the mass lost as vapour to the Langmuir equation, to establish vapour pressure as a  
52 function of temperature.<sup>31</sup> Compound **1** was shown to be more volatile at lower temperatures, and to  
53 have 1 Torr of vapour pressure at 131 °C (using benzoic acid as a standard). Compound **2** had a  
54 slightly lower volatility, and gave 1 Torr of vapour pressure at 139 °C. However, both of these  
55 compounds can be expected to give reasonably high vapour pressures at normal bubbler temperatures,  
56 and the similarity of the slopes of their evaporation curves suggests that they experience similar  
57 intermolecular attraction during evaporation.  
58  
59  
60

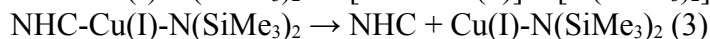
1  
2  
3  
4  
5  
6 Since the TGA of **1** showed no thermal decomposition, a thermal “delivery stability” test was  
7 performed to determine the long-term stability of this compound at reasonable bubbler temperatures. It  
8 is desirable for ALD precursors to demonstrate stability under bubbler conditions to ensure predictable  
9 and consistent vapour pressures delivered with each pulse. The thermal stress test used a stainless steel  
10 vessel which was heated in an isothermal oven. Samples were taken using a glovebox every 48 h for 2  
11 weeks, and the samples were analysed by TGA and  $^1\text{H}$  NMR. A 90 °C oven temperature was chosen as  
12 this was the delivery temperature in plasma-enhanced (PE) ALD experiments described below. The  
13 TGA showed an increasing trend in residual mass from 2 % to 3 % over two weeks, which is an  
14 excellent thermal stability at delivery temperatures. The  $^1\text{H}$  NMR spectra measured on day 1 and day  
15 14 both showed only peaks for **1**. This delivery stability test was repeated using an oven temperature of  
16 130 °C. Sampling over two weeks showed the residueEnergy dispersive X-ray spectroscopy (EDS)  
17 showed the resulting material to be copper metal, with some minor carbon impurities (<5%).al mass  
18 increasing from 1 % to 3 %. Again,  $^1\text{H}$  NMR spectra corroborated the excellent thermal stability  
19 displayed at 130 °C. A delivery stability test was not performed for **2**, as decomposition was evident  
20 from preliminary TGA.  
21  
22  
23

24  
25 Compound **1** was successful at depositing copper metal using PE-ALD. A typical experiment saw 0.3 -  
26 0.5 g of **1** loaded into a Beneq TFS 200 reactor equipped with a capacitively coupled plasma source.  
27 The substrate was heated to 225 °C and the precursor was heated to 90 °C to ensure sufficient vapour  
28 of **1** reaching the deposition chamber. A pulse of **1** was followed by a 3 s purge with nitrogen gas,  
29 alternating with a 6 s pulse of hydrogen plasma and a second purge. Varying the pulse length of **1**  
30 allowed a saturation curve to be collected (Figure 3). The growth rate plateaued at 0.2 Å/cycle after 4  
31 seconds, corresponding to about 10 % of a monolayer of Cu. ALD-grown copper has been reported  
32 with growth rates of 0.12 Å/cycle (on Ru),<sup>32</sup> 0.18Å/cycle,<sup>33</sup> and 0.90 Å/cycle<sup>34</sup>, showing this growth  
33 rate to be within this range. Energy dispersive X-ray spectroscopy (EDS) showed the resulting material  
34 to be copper metal, with some minor carbon impurities (<5%). Since the thicknesses were measured  
35 using the k-ratios from EDS, the growth from 1 s and 2 s pulse lengths gave no thickness. However,  
36 scanning electron microscopy showed nucleation of copper nanoparticles (Figure 4). It was obvious  
37 that the deposited copper was crystalline over all deposition ranges, and X-ray diffraction showed  
38 typical copper signals, and demonstrated the absence of copper oxide crystalline phases. Many of the  
39 deposited films were too thin and non-continuous for resistivity measurements, but the film deposited  
40 with a 5 s pulse had a thickness of 35 nm and gave a resistivity of 11.23  $\mu\Omega\cdot\text{cm}$ . This is not unusual for  
41 the deposition of copper metal on silicon: the high mobility of copper atoms on the growing surface  
42 result in an island growth mechanism that causes non-uniformity.  
43  
44  
45  
46

47 Compound **2** could not be used under any tested conditions as a copper metal precursor. The resulting  
48 depositions were not metallic, but showed an interference colour pattern similar to non-uniform  
49 deposition of a transparent material. A typical “blank” experiment was performed where by the  
50 hydrogen pulse was not activated to plasma. No film growth was observed during this experiment for  
51 either **1** or **2**. The difference in the deposition results between **1** and **2** was attributed to the NHC, since  
52 the rest of the molecule is unchanged.  
53  
54

55 DFT calculations were carried out on these precursors in the gas phase and adsorbed to model copper  
56 surfaces. The computed structures were in good agreement with the X-ray structural analysis, with all  
57 bond lengths agreeing within 5 pm (Table 1). The dissociation energy of each ligand from the copper  
58 centre was calculated to determine which bond was likely to break upon chemisorption at a copper  
59  
60

1  
2  
3  
4 surface. The chemical equations considered were heterolysis of the amide bond (1), homolysis of the  
5 amide bond (2), and loss of the NHC (3):  
6



12  
13 In compounds **1** and **2**, it was found that the copper-nitrogen bond (Eqs. 1 and 2) was much stronger  
14 than the copper-C bond to NHC (Eq. 3), (646 and 428 kJ/mol vs. 293 kJ/mol for **1**; 636 and 427 kJ/mol  
15 vs. 298 kJ/mol for **2**). Thus, the amide will remain bound to the Cu atom during adsorption, which  
16 likely forms new Cu-Cu bonds with the surface, while the carbene may dissociate from the adsorbing  
17 molecule and bond separately to the surface or evaporate.  
18

19  
20 The precursors were brought to a model copper surface and relaxed with DFT in order to determine  
21 their adsorption energy ( $\Delta E_{ad}$ ). In both cases, the Cu atom of the precursor optimized to a distance of  
22 5.4 Å from the nearest surface Cu atom (Figure 5). The precursor contacted the surface via the alkyl  
23 substituent of the  $\text{N}(\text{SiMe}_3)_2$ , with a shortest Cu-H distance of 2.4 Å to the nearest surface Cu atom.  
24 These are non-bonded distances, indicative of molecular physisorption. We can see from the DFT  
25 energetics (Table 2) that the precursors have weak molecular adsorption to the surface for both **1** and **2**,  
26 although there is some uncertainty in this value because of the poor description of physisorption by  
27 DFT. Explicit inclusion of van der Waals interactions in the DFT functional may give a more accurate  
28 value<sup>35,36</sup>, but the use of such functionals for organometallic reagents adsorbed onto metal surfaces is  
29 not yet well established and hence is beyond the scope of our study.<sup>37</sup>  
30  
31

32  
33 It appears that steric hindrance in the  $\text{N}(\text{SiMe}_3)_2$  moiety prevents the coordinatively unsaturated Cu, C  
34 and N atoms of the precursor from coming close to the surface (Figure 5). The only pathway to  
35 chemisorption is therefore through dissociation of the precursor at the Cu-NHC bond. The adsorption  
36 energies show that the carbene of **1** and **2** can adsorb to the smooth surface with comparable energies  
37 (Table 2). For a smooth copper surface, the adsorption energies are low and - consistent with this - the  
38 computed distances indicate that no chemical bonds are formed to the Cu surface. However, when a  
39 rough surface (modeled by an additional copper(I) adatom) is considered, the NHC ligands bind to this  
40 surface site with adsorption energies that are comparable to those of the Cu- $\text{N}(\text{SiMe}_3)_2$  moiety. The  
41 DFT data do not show any significant difference between the saturated carbene (from **1**) and  
42 unsaturated carbene (from **2**) in terms of energetics of dissociation or adsorption during the Cu pulse.  
43 This indicates that differences between the ALD chemistry of these two precursors arise after the Cu  
44 pulse, probably during the plasma  $\text{H}_2$  pulse. Further studies are under way to determine the differences  
45 in the surface chemistry of these two compounds.  
46  
47  
48

## 49 Conclusion

50  
51 Two novel NHC-containing compounds 1,3-diisopropyl-imidazolin-2-ylidene copper  
52 hexamethyldisilazide (**1**) and 4,5-dimethyl-1,3-diisopropyl-imidazol-2-ylidene copper  
53 hexamethyldisilazide (**2**) were synthesized and structurally characterized. Compound **1** was found to  
54 have excellent volatility and thermal stability over an extended period of time. It was successfully  
55 employed as an ALD precursor using hydrogen plasma as a reducing agent. The deposited films had a  
56 growth rate of 0.2 Å/cycle and were crystalline. The films showed good resistivity.  
57  
58  
59  
60

Compound **2** showed excellent volatility but poorer thermal stability than **1**. Under similar conditions to the ALD of **1**, it did not afford a copper metal film. DFT studies of both precursors showed good dissociative chemisorption to a copper surface, with cleavage of the precursor at the carbene-copper bond, indicating similar surface chemistry during the Cu precursor pulse in ALD.

**Acknowledgement:** STB would like to acknowledge funding from NSERC Discovery and GreenCentre Canada. GD and SDE would like to acknowledge funding from Science Foundation Ireland under the ALDesign project (09.IN1.I2628) <http://www.tyndall.ie/aldesign>. GPAY and ERS acknowledge NSF-CRIF 1048367. MK, ML, MR thank the Finnish Centre of Excellence in Atomic Layer Deposition.

## Experimental

**General Considerations:** All manipulations involving the synthesis and handling of copper(I) compounds were performed in an MBraun Labmaster™ 130 Dry box (mBraun, Stratham, NH, U.S.A.) under a nitrogen atmosphere. NMR spectra were recorded on a 400 MHz Bruker AMX spectrometer. NMR spectra were measured in C<sub>6</sub>D<sub>6</sub> and were referenced against residual protonated solvent. 1,3-diisopropyl-imidazolin-2-ylidene copper chloride was prepared from a literature method substituting imidazolinium tetrafluoroborate for imidazolinium chloride.<sup>38</sup> 4,5-dimethyl-1,3-diisopropyl-imidazol-2-ylidene copper chloride was prepared by following established literature methods for NHC CuCl.<sup>39</sup> 4,5-dimethyl-1,3-diisopropyl-imidazol-2-ylidene<sup>40</sup> and 1,3-diisopropyl-imidazolinium chloride<sup>41</sup> were prepared according to literature. The diethyl ether adduct of lithium hexamethyldisilazide was prepared according to literature.<sup>42</sup> All reagents were purchased from Sigma Aldrich (Oakville, Ontario, Canada) and used as received. All solvents were purchased as ACS grade and purified from an Mbraun Solvent Purifier System.

**1,3-diisopropyl-imidazolin-2-ylidene copper hexamethyldisilazide (1):** 1,3-diisopropyl-imidazolin-2-ylidene copper chloride (4.456 g, 17.52 mmol) was partially dissolved in 130 mL of toluene and cooled in the glove box freezer to -35 °C before use. In a separate flask, Et<sub>2</sub>O·LiN(SiMe<sub>3</sub>)<sub>2</sub> (4.248 g, 17.6 mmol) was dissolved in 70 mL of toluene. The amide solution was added dropwise over the course of a hour and the cloudy solution was stirred for 24 h, after which the solution was filtered and the insoluble material was washed with 3 × 10 mL of toluene. The washings were combined with the filtrate and volatiles were stripped off under reduced pressure. The crude product was purified by sublimation (T<sub>sub</sub> = 90 °C, 35 mTorr) using a dry ice/acetone cold finger and collected as a colourless solid (6.322 g, 95 %); m.p. 49-51 °C. <sup>1</sup>H NMR (400 MHz, C<sub>6</sub>D<sub>6</sub>): δ 4.46 [sept, 2H, NCH(CH<sub>3</sub>)<sub>2</sub>], δ 2.50 [s, 4H, N(CH<sub>2</sub>)<sub>2</sub>N], δ 0.81 [d, 12H, NCH(CH<sub>3</sub>)<sub>2</sub>], δ 0.54 [s, 18H, N(Si(CH<sub>3</sub>)<sub>3</sub>)<sub>2</sub>]. <sup>13</sup>C NMR (100 MHz, C<sub>6</sub>D<sub>6</sub>): δ 200.39 [NCN], δ 51.16 [NCH(CH<sub>3</sub>)<sub>2</sub>], δ 41.91 [N(CH<sub>2</sub>)<sub>2</sub>N], δ 20.68 [NCH(CH<sub>3</sub>)<sub>2</sub>], δ 7.20 [N(Si(CH<sub>3</sub>)<sub>3</sub>)<sub>2</sub>]. HRMS (EI) m/z calcd for C<sub>15</sub>H<sub>36</sub>N<sub>3</sub>Si<sub>2</sub>Cu M<sup>+</sup> 377.1744, found 377.1763.

**4,5-dimethyl-1,3-diisopropyl-imidazol-2-ylidene copper hexamethyldisilazide (2):** Compound **2** was prepared in an analogous manner as compound **1** substituting: 4,5-dimethyl-1,3-diisopropyl-imidazol-2-ylidene copper chloride (0.518 g, 1.85 mmol) partially dissolved in 15 mL of toluene, Et<sub>2</sub>O·LiN(SiMe<sub>3</sub>)<sub>2</sub> (0.449 g, 1.86 mmol) dissolved in 8 mL of toluene. Compound **2** was isolated by sublimation (T<sub>sub</sub> = 95 °C, 25 mTorr) as a white solid (0.630 g, 84.0%); m.p. 119 °C. <sup>1</sup>H NMR (400 MHz, C<sub>6</sub>D<sub>6</sub>): δ 4.08 [sept, 2H, NCH(CH<sub>3</sub>)<sub>2</sub>], δ 1.41 [s, 6H, N(CCH<sub>3</sub>)<sub>2</sub>N], δ 1.37 [d, 12H, NCH(CH<sub>3</sub>)<sub>2</sub>], δ 0.59 [s, 18H, N(Si(CH<sub>3</sub>)<sub>3</sub>)<sub>2</sub>]. <sup>13</sup>C NMR (100 MHz, C<sub>6</sub>D<sub>6</sub>): δ 173.21 [NCN], δ 123.08 [N(CCH<sub>3</sub>)<sub>2</sub>N], δ 50.67 [NCH(CH<sub>3</sub>)<sub>2</sub>], δ 24.02 [NCH(CH<sub>3</sub>)<sub>2</sub>], δ 8.80 [N(CCH<sub>3</sub>)<sub>2</sub>N], δ 7.12 [N(Si(CH<sub>3</sub>)<sub>3</sub>)<sub>2</sub>]. HRMS (EI)

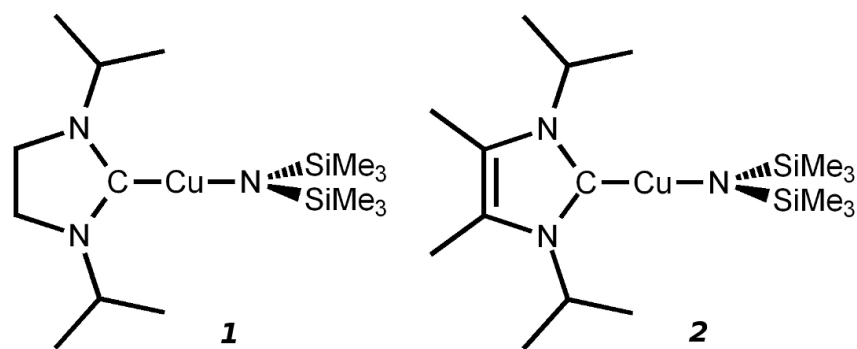


m/z calcd for  $C_{17}H_{38}N_3Si_2Cu M^+$  403.1900, found 403.1924.

**Computational Study:** The ground state electronic wave function of each molecule was calculated self-consistently within Kohn-Sham DFT using the TURBOMOLE suite of quantum chemical programs.<sup>43,44</sup> The Perdew-Burke-Ernzerhof functional<sup>45</sup> with the resolution-of-the-identity approximation<sup>46,47</sup> and an all-electron valence double-zeta with polarization def-SV(P) basis set<sup>48</sup> was considered the most suitable level of calculation. No basis set superposition error correction was required for a basis of this size. An even larger def-TZV(P)<sup>46</sup> basis set gives reaction energies that agree to less than 10%, but are an order of magnitude more costly in computational time. Structures are relaxed using DFT with no constraints, except to stop adsorbates drifting towards the edge of the cluster. All the neutral Cu(I) carbene precursor molecules are closed shell compounds. A 55 copper atom cluster of  $C_{3v}$  symmetry, which is in the shape of a coin ( $Cu_{55}$ ), is used as a model of the (1 1 1) surface to see the effect of adsorption of various copper precursors. A rough surface has been generated by the addition of one Cu atom ( $Cu_{56}$ ). The copper coin is an open shell system with the HOMO LUMO energy difference of <2 kJ/mol. NPA<sup>49</sup> has been carried out in order to obtain a qualitative understanding of the charge distribution .

**Crystallography:** X-ray structural analysis: Crystals were selected and mounted on plastic mesh using viscous oil flash-cooled to the data collection temperature. Data were collected on a Brüker-AXS APEX CCD diffractometer with graphite-monochromated Mo- $K\alpha$  radiation ( $\lambda=0.71073 \text{ \AA}$ ). Unit cell parameters were obtained from 60 data frames,  $0.3^\circ \omega$ , from three different sections of the Ewald sphere. The systematic absences in the data and the unit cell parameters were uniquely consistent to  $P2_1/n$ . The data-sets were treated with absorption corrections based on redundant multiscan data. The structures were solved using direct methods and refined with full-matrix, least-squares procedures on  $F^2$ . In **1**, one isopropyl and both trimethylsilyl groups, and in **2**, one trimethylsilyl group, were rotationally disordered with **1**(isopropyl:trimethyl:trimethyl):**2**(isopropyl)::88/12:63/37:60/40:51/49 refined site occupancies. Chemically equivalent bond distances and angles in the disordered group were constrained to average values and with equal atomic displacement atomic parameter restraints on equivalent atoms. All atoms were treated in **1** were treated with rigid bond restraints. All non-hydrogen atoms were refined with anisotropic displacement parameters. All hydrogen atoms were treated as idealized contributions. Atomic scattering factors are contained in the SHELXTL 6.12 program library (Sheldrick, G.M. 2008. Acta Cryst. A64, 112-122).

**PE ALD:** Coppe thin films were deposited on silicon (100) substrates in a Beneq TFS-200 ALD-reactor, capable of depositing on 200 mm wafers, with a remote plasma configuration.<sup>14b</sup> Plasma was generated with capacitive coupling with a 13.56 MHz rf power source. The plasma power was 170 W. The distance between the substrate and the grid, which was the bottom electrode, was 4 cm. Plasma activated hydrogen was used as the reducing agent. Hydrogen gas (99.999%, AGA) was mixed with argon (99.999%, AGA) to ensure plasma ignition. In general, the hydrogen flow was 20 sccm and the argon plasma gas flow 140 sccm. The hydrogen flow was not pulsed because no reaction between the precursor and molecular hydrogen was noticed at the applied growth temperatures. Argon carrier gas flow was typically 330 sccm. Gases were purified on-site before mixing with Aeronex GateKeeper and Entegris GateKeeper purifiers.



**Scheme 1.** The structures of 1,3-diisopropyl-imidazolin-2-ylidene copper hexamethyldisilazide (**1**) and 4,5-dimethyl-1,3-diisopropyl-imidazol-2-ylidene copper hexamethyldisilazide (**2**).

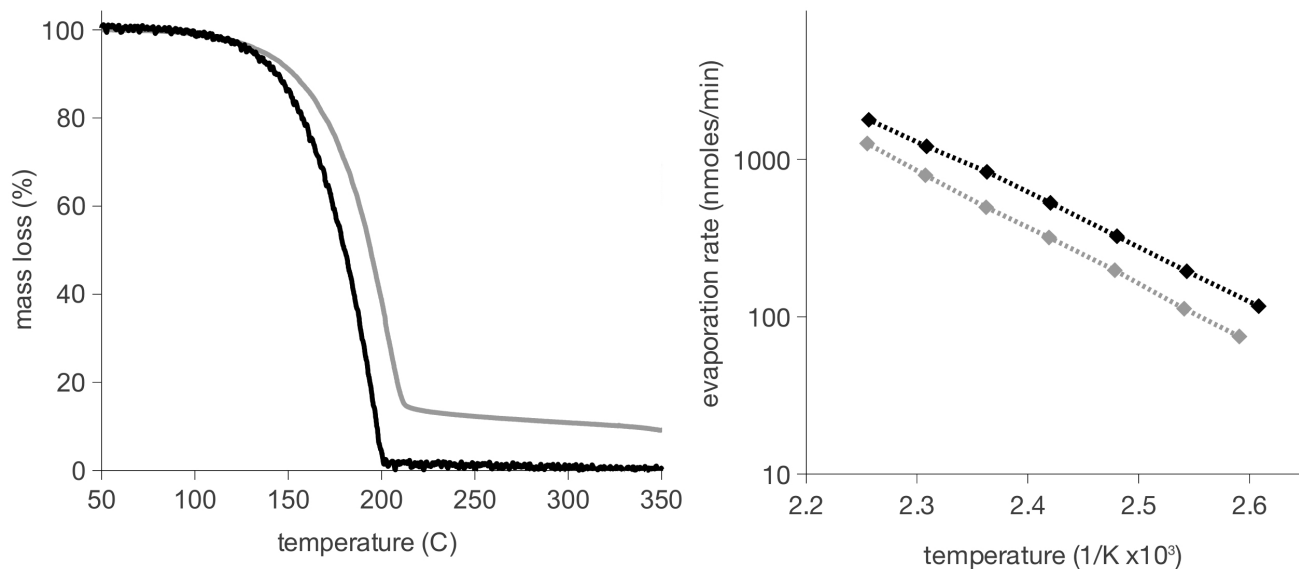


**Figure 1.** Thermogravimetric analyses and evaporation rates of **1** (black) and **2** (grey) run at 10 °C/min ramp rate, with 10 °C increments for the stepped isotherm used to determine evaporation rate.

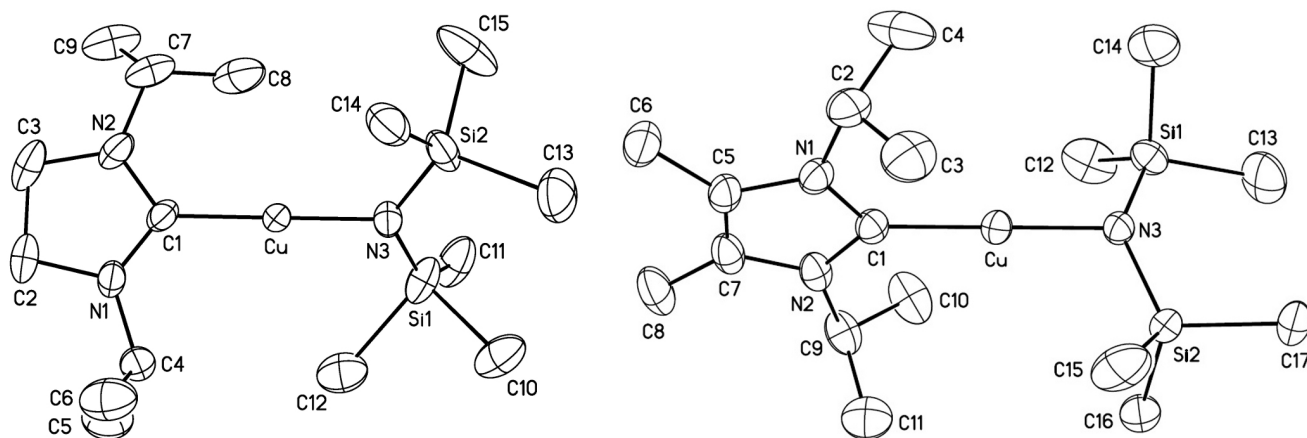


**Figure 2.** The X-ray structure of **1** (left) and **2**, (right), with H-atoms and minor disordered contributions omitted for clarity and at 30 % probability ellipsoids.

**Table 1.** Selected bond lengths and bond angles for the structures of **1** and **2**.

Compound 1			Compound 2		
Selected Bond Lengths (Å)					
	experimental	computational		experimental	computational
Cu-N3	1.836(4)	1.869	Cu-N3	1.870(2)	1.869
Cu-C1	1.870(5)	1.897	Cu-C1	1.881(2)	1.897
N1-C1	1.330(7)	1.356	N1-C1	1.360(3)	1.367
N1-C2	1.472(7)	1.470	N1-C5	1.404(3)	1.397
N2-C1	1.336(6)	1.356	N2-C1	1.365(3)	1.372
N2-C3	1.444(9)	1.471	N2-C7	1.394(3)	1.399
Si1-N3	1.680(6)	1.742	N3-Si2	1.692(2)	1.742
Si2-N3	1.701(5)	1.742	N3-Si1	1.697(2)	1.741
C2-C3	1.531(12)	1.538	C5-C7	1.338(4)	1.384
Selected Bond Angles (°)					
N3-Cu-C1	179.2(2)	178.3	N3-Cu-C1	178.60(9)	175.5
C1-N1-C2	114.2(5)	112.1	C1-N1-C5	111.0(2)	111.4
C1-N2-C3	114.7(6)	112.5	C1-N2-C7	111.6(2)	111.4
Si1-N3-Si2	128.2(3)	128.2	Si2-N3-Si1	131.26(13)	128.1
Si1-N3-Cu	116.5(3)	116.0	Si1-N3-Cu	113.19(11)	113.0
Si2-N3-Cu	115.3(3)	115.1	Si2-N3-Cu	111.21(11)	113.0
N1-C1-N2	106.6(5)	107.9	N1-C1-N2	103.9(2)	104.5
N1-C1-Cu	127.0(4)	128.0	N1-C1-Cu	127.26(19)	130.6
N2-C1-Cu	126.3(5)	128.0	N2-C1-Cu	128.88(19)	130.6

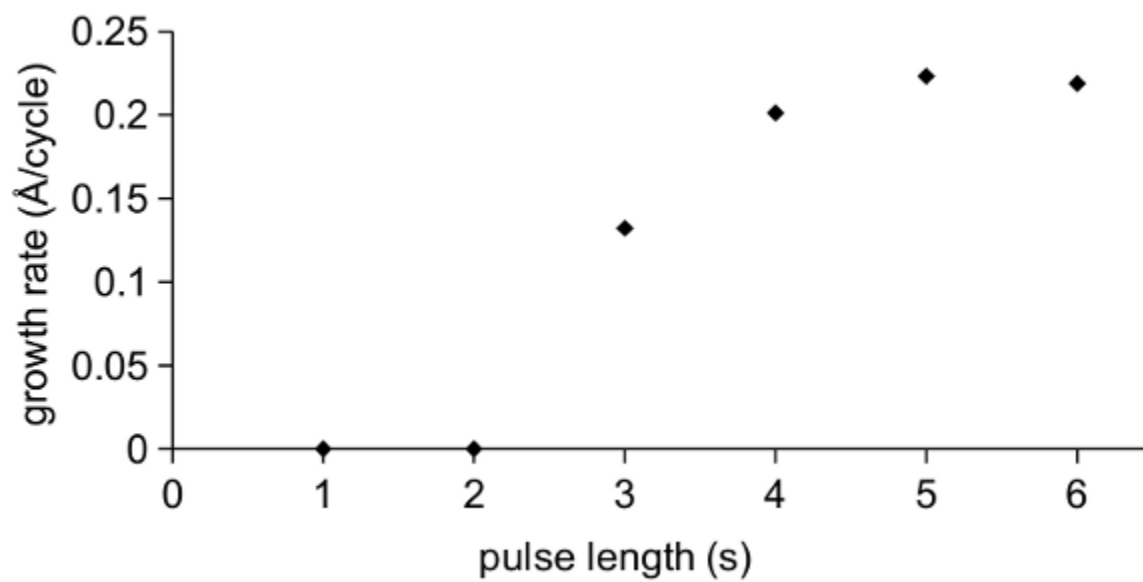


**Figure 3.** ALD saturation curve for **1** as the pulse length of **1** was varied.

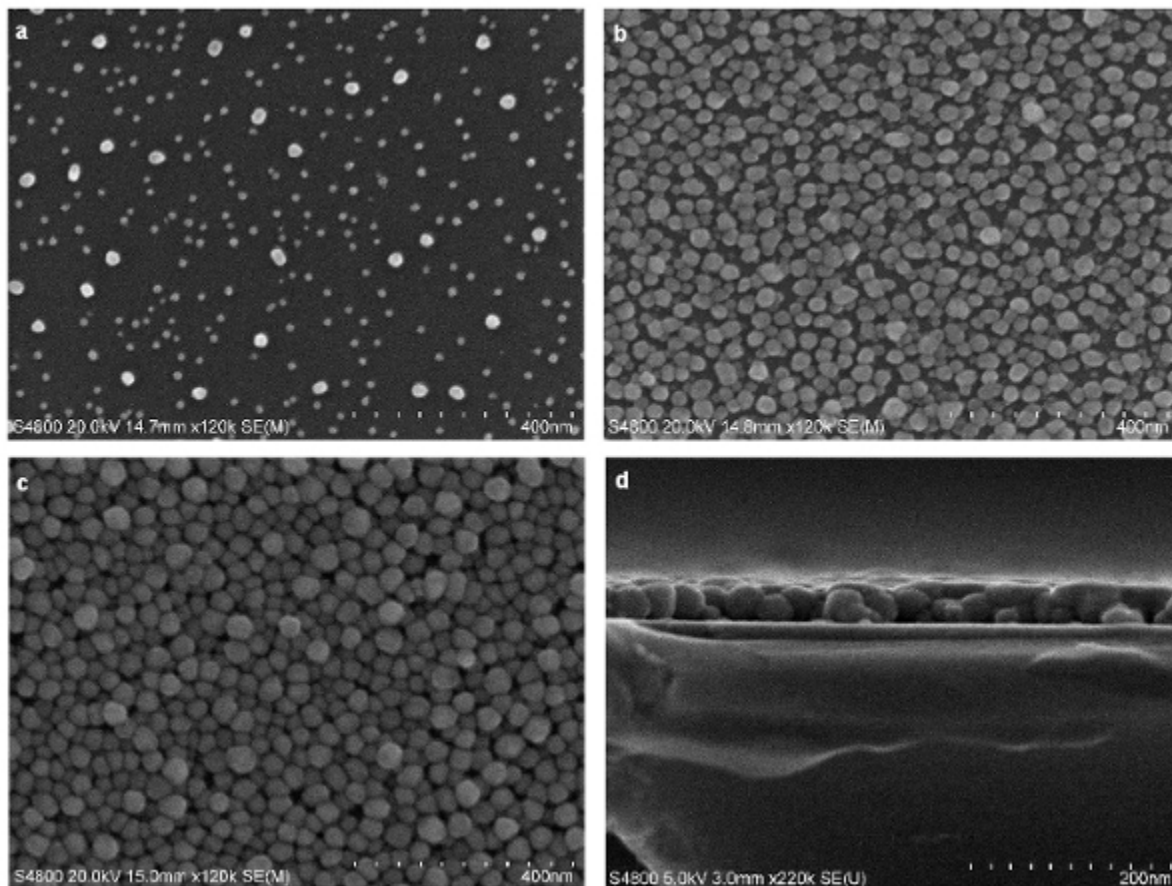


**Figure 4.** Scanning electron micrographs of deposited copper films. a) Plan view of copper nanoparticles deposited using a 1 s pulse length. b) Plan view of crystalline copper deposited using a 4 s pulse length. c) Plan view of crystalline copper deposited using a 6 s pulse length. d) a profile of crystalline copper deposited using a 6 s pulse length.

**Table 2:** Computed adsorption energy  $\Delta E_{\text{ad}}$  (kJ/mol) of the precursors and their probable by-products on two surface models - Cu<sub>55</sub> with a smooth (111) surface and Cu<sub>56</sub> with one extra atom making the surface rough. Values for physisorption are in brackets because of the limited accuracy of the PBE functional in describing van der Waals interactions.

Adsorbate	Surface model	Structure	Compound 1	Compound 2
Cu(NHC)[N(SiMe <sub>3</sub> ) <sub>2</sub> ]	smooth Cu <sub>55</sub>	Fig 5a	(-174)	(-174)
NHC	smooth Cu <sub>55</sub>	Fig 5d	(-61)	(-83)
NHC	rough Cu <sub>56</sub>	Fig 5c	-820	-806
NHC (dimer)	smooth Cu <sub>55</sub>	-	(-113)	(-101)
Cu(I)(NHC) <sup>+</sup>	smooth Cu <sub>55</sub>	Fig 5c	-364	-353
[N(SiMe <sub>3</sub> ) <sub>2</sub> ] <sup>-</sup>	smooth Cu <sub>55</sub>	-		-378
[N(SiMe <sub>3</sub> ) <sub>2</sub> ] <sup>-</sup>	rough Cu <sub>56</sub>	Fig 5b		-385
Cu(I)[N(SiMe <sub>3</sub> ) <sub>2</sub> ]	smooth Cu <sub>55</sub>	Fig 5b		-308



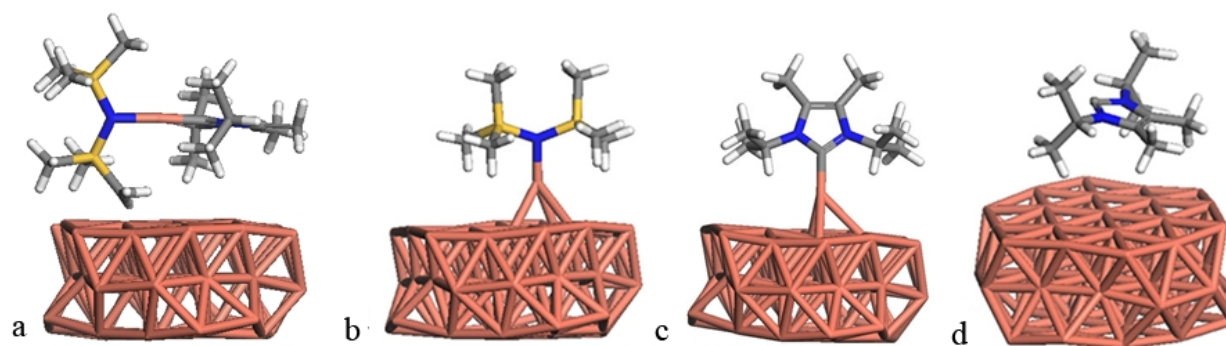


**Figure 5.** Optimized geometries of (a) **2** molecularly physisorbed on a smooth Cu (111) surface; (b)  $\text{CuN}(\text{SiMe}_3)_2$  chemisorbed on the smooth surface; (c) NHC from **2** chemisorbed onto a rough surface; (d) NHC from **2** physisorbed on the smooth surface.

- 1  
2  
3  
4  
5  
6  
7  
8  
9  
10  
11  
12  
13  
14  
15  
16  
17  
18  
19  
20  
21  
22  
23  
24  
25  
26  
27  
28  
29  
30  
31  
32  
33  
34  
35  
36  
37  
38  
39  
40  
41  
42  
43  
44  
45  
46  
47  
48  
49  
50  
51  
52  
53  
54  
55  
56  
57  
58  
59  
60
- 1 *International Technology Roadmap for Semiconductors*; **2011**; <http://www.itrs.net/>.
- 2 a) Chen, T. Y.; Omnes, L.; Vaisserman, J.; Doppelt, P. *Inorg. Chim. Acta.* **2004**, 357, 1299, b)
- 3 Bollmann, D.; Merkel, R.; Klumpp, A. *Microelectron. Eng.* **1997**, 37-8, 105, c) Lagalante, A. F.;
- 4 Hansen, B. N.; Bruno, T. J.; Sievers, R. E. *Inorg. Chem.* **1995**, 34, 5781 d) Wenzel, T. J.; Williams, E.
- 5 J.; Haltiwanger, R. C.; Sievers, R. E. *Polyhedron* **1985**, 4, 369.
- 6 Park, K. H.; Marshall, W. J. *J. Am. Chem. Soc.* **2005**, 127, 9330.
- 7 a) Li, Z. W.; Rahtu, A.; Gordon, R. G. *J. Electrochem. Soc.* **2006**, 153, C787, b) Li, Z. W.; Barry,
- 8 S. T.; Gordon, R. G. *Inorg. Chem.* **2005**, 44, 1728, c) Lim, B. S.; Rahtu, A.; Gordon, R. G. *Nat. Mater.*
- 9 **2003**, 2, 749, c) Lim, B. S.; Rahtu, A.; Park, J. S.; Gordon, R. G. *Inorg. Chem.* **2003**, 42, 7951.
- 10 Coyle, J. P.; Monillas, W. H.; Yap, G. P. A.; Barry, S. T. *Inorg. Chem.* **2008**, 47, 683.
- 11 Park, J. W.; Jang, H. S.; Kim, M.; Sung, K.; Lee, S. S.; Chung, T.; Koo, S.; Kim, C. G.; Kim, Y.
- 12 *Inorg. Chem. Commun.* **2004**, 7, 463.
- 13 Grushin, V. V.; Marshall, W. J. *Adv. Synth. Catal.* **2004**, 346, 1457.
- 14 Knoop, H. C. M.; Langereis, E.; van de Sanden, M. C. M.; Kessels, W. M. M. *J.*
- 15 *Electrochem. Soc.* **2010**, 157, 12, G241.
- 16 Gambarotta, S.; Bracci, M.; Floriani, C.; Chiesi-Villa, A.; Guastini, C. *J. Chem. Soc., Dalton*
- 17 *Trans.* **1987**, 1883.
- 18 Tsuda, T.; Watanabe, K.; Miyata, K.; Yamamoto, H.; Saegusa, T. *Inorg. Chem.* **1981**, 20, 2728.
- 19 Gaillard, S.; Cazin, C. J.; Nolan, S. P. *Acc. Chem. Res.* **2012**, 45, 778, and references therein.
- 20 a) Goj, L. A.; Blue, E. D.; Delp, S. A.; Gunnoe, T. B.; Cundar, T. R.; Pierpont, A. W.; Petersen,
- 21 J. L.; Boyle, P. D. *Inorg. Chem.* **2006**, 45, 9032, b) Goj, L. A.; Blue, E. D.; Munro-Leighton, C.;
- 22 Gunnoe, T. B.; Petersen, J. L. *Inorg. Chem.* **2005**, 44, 8647.
- 23 Mankad, N. P.; Laitar, D. S.; Sadighi, J. P. *Organometallics* **2004**, 23, 3369.
- 24 a) Niskanen, A.; Hatanpää, T.; Arstila, K.; Leskelä, M.; Ritala, M. *Chem. Vap. Deposition* **2007**, 13,
- 25 408, b) Kariniemi, M.; Niinistö, J.; Hatanpää, T.; Kemell, M.; Sajavaara, T.; Ritala, M.; Leskelä, L.
- 26 *Chem. Mater.* **2011**, 23, 2901
- 27 Denk, M. K.; Thadani, A.; Hantano, K.; Lough, A. J. *Angew. Chem. Int. Ed.* **1997**, 36, 2607
- 28 Jain, A.; Chi, K. -M.; Kodas, T. T.; Hampden-Smith, M. J. *J. Electrochem. Soc.* **1993**, 140, 1434
- 29 a) Nyburg, S. C.; Parkins, A. W.; Sidi-BouMedine, M. *Polyhedron* **1993**, 12, 1119, b) Melzer, M.
- 30 M.; Mossin, S.; Day, X.; Bartell, A. M.; Kapoor, P.; Meyer, K.; Warren, T. H. *Angew. Chem. Int. Ed.*
- 31 **2010**, 49, 904, c) Harkins, S. B.; Mankad, N. P.; Miller, A. J. M.; Szilagy, R. K.; Peters, J. C. *J.*
- 32 *Am. Chem. Soc.* **2008**, 130, 3478
- 33 James, A. M.; Laxman, R. K.; Fronczek, F. R.; Maverick, A. W. *Inorg. Chem.* **1998**, 37, 3785
- 34 Elliott, S. D. *Semicond. Sci. Tech.* **2012**, 27, 074008.
- 35 Widjaja, Y.; Musgrave, C. B. *J. Chem. Phys.* **2002**, 117, 1931.
- 36 Jeloica, L.; Esteve, A.; Rouhani, M. D.; Esteve, D. *Appl. Phys. Lett.* **2003**, 83, 542.
- 37 Li, J.; Wu, J.; Zhou, C.; Han, B.; Lei, X.; Gordon, R.; Cheng, H. *Int. J. Quantum Chem.* **2009**,
- 38 109, 756.
- 39 Kwon, J.; Saly, M.; Halls, M. D.; Kanjolia, R. K.; Chabal, Y. J. *Chem. Mater.* **2012**, 24, 1025.
- 40 a) Mårtensson, P.; Larsson, K.; Carlsson, J.-O. *Appl. Surf. Sci.* **1998**, 136, 137, b) Mårtensson,
- 41 P.; Larsson, K.; Carlsson, J.-O. *Applied Surface Science* **1999**, 148, 9, c) Mårtensson, P.; Larsson, K.;
- 42 Carlsson, J.-O. *Appl. Surf. Sci.* **2000**, 157, 92.
- 43 Dai, M.; Kwon, J.; Halls, M. D.; Gordon, R. G.; Chabal, Y. J. *Langmuir* **2010**, 26, 3911.
- 44 Orimoto, Y.; Toyota, A.; Furuya, T.; Nakamura, H.; Uehara, M.; Yamashita, K.; Maeda, H. *Ind.*
- 45 *Eng. Chem. Res.* **2009**, 48, 3389.
- 46 Machado, E.; Kaczmarski, M.; Ordejón, P.; Garg, D.; Norman, J.; Cheng, H. *Langmuir* **2005**,
- 47 21, 7608.
- 48 Dey, G.; Elliott, S. D. *J. Phys. Chem. A* **2012**, 116, 8893.
- 49 Lee, B. H.; Hwang, J. K.; Nam, J. W.; Lee, S. U.; Kim, J. T.; Koo, S.-M.; Baunemann, A.;

- 1  
2 Fischer, R. A.; Sung, M. M. *Angew. Chem. Int. Ed.* **2009**, *48*, 4536.  
3 30 a) Lin, J. C. Y.; Huang, R. T. W.; Lee, C. S.; Bhattacharyya, A.; Hwang, W. S.; Lin, I. J. B.  
4 *Chem. Rev.* **2009**, *109*, 3561, b) An, D.; Wang, J.; Dong, T.; Yang, Y.; Wen, T.; Zhu, H.; Lu, X.; Wang,  
5 Y. *Eur. J. Inorg. Chem.* **2010**, 4506  
6  
7 31 Kunte, G. V.; Shivashankar, S. A.; Umarji, A. M. *Meas. Sci. Technol.* **2008**, *19*, 025704.  
8 32 Park, K.-M.; Kim, J.-K.; Han, B.; Lee, W.-J.; Kim, J.; Shin, H.-K. *Microelectron. Eng.* **2012**,  
9 89, 27.  
10 33 Niskanen, A.; Rahtu, A.; Sajavaara, T.; Arstila, K.; Ritala, M.; Leskela, M. *J. Electrochem. Soc.*  
11 **2005**, *152*, G25.  
12 34 Li, Z.; Rahtu, A.; Gordon, R. G. *J. Electrochem Soc.* **2006**, *153*, C787  
13 35 Lundqvist, B. I.; Andersson, Y.; Shao, H.; Chan, S.; Langreth, D. C. *Int. J. Quantum Chem.*  
14 **1995**, *56*, 247.  
15 36 Ruiz, V. G.; Liu, W.; Zojer, E.; Scheffler, M.; Tkatchenko, A. *Phys. Rev. Lett.* **2012**, *108*,  
16 146103.  
17 37 Marom, N.; Tkatchenko, A.; Rossi, M.; Gobre, V. V.; Hod, O.; Scheffler, M.; Kronik, L. J.  
18 *Chem. Theory Comput.* **2011**, *7*, 3944.  
19 38 Dubinina, G.G.; Furutachi, H.; Vivic, D. A. *J. Am. Chem. Soc.* **2008**, *130*, 8600.  
20 39 Díez-González, S.; Escudero-Adán, E. C.; Benet-Buchholz, J.; Stevens, E. D.; Slawin, A. M. Z.;  
21 Nolan, S. P. *Dalt. Trans.* **2010**, *39*, 7595.  
22 40 Kuhn, N.; Kratz, T. *Synthesis* **1993**, 561.  
23 41 Bittermann, A.; Baskakov, D.; Herrmann, W. A. *Organometallics* **2009**, *28*, 5107.  
24 42 Lappert, M. F.; Slade, M. J.; Singh A.; Atwood, J. L.; Rogers, R. D.; Shakir, R. *J. Am. Chem.*  
25 *Soc.* **1983**, *105*, 302.  
26 43 Schafer, A.; Huber, C.; Ahlrichs, R. *J. Chem. Phys.* **1994**, *100*, 5829.  
27 44 Ahlrichs, R.; Bär, M.; Häser, M.; Horn, H.; Kölmel, C. *Chem. Phys. Lett.* **1989**, *162*, 165.  
28 45 Perdew, J. P.; Burke, K.; Ernzerhof, M. *Phys. Rev. Lett.* **1996**, *77*, 3865.  
29 46 Eichkorn, K.; Weigend, F.; Treutler, O.; Ahlrichs, R. *Theor. Chim. Acta.* **1997**, *97*, 119.  
30 47 Sierka, M.; Hoge Kamp, A.; Ahlrichs, R. *J. Chem. Phys.* **2003**, *118*, 9136.  
31 48 Schafer, A.; Horn, H.; Ahlrichs, R. *J. Chem. Phys.* **1992**, *97*, 2571.  
32 49 Cioslowski, J. *J. Am. Chem. Soc.* **1989**, *111*, 8333.  
33  
34  
35  
36  
37  
38  
39  
40  
41  
42  
43  
44  
45  
46  
47  
48  
49  
50  
51  
52  
53  
54  
55  
56  
57  
58  
59  
60